DE-13-C046

Use of Numerical Simulation and Optimization to Analyze the Design and Performance of a Chilled Water Thermal Storage Tank

Reza Ghias, D.Sc. *ASHRAE Member*
Yue Xu *Associate ASHRAE Member*
Richard Ellison, PE *ASHRAE Member*
Curt Eisenhower, PE *ASHRAE Member*

ABSTRACT

Chilled water thermal storage tanks are an efficient and economic option in HVAC design. The sensible cooling capacity, which is typically generated and stored during lower demand periods, can serve many purposes such as reducing energy costs during peak demands, backing up cooling capacity during a power outage, and suppressing fire during a fire accident. The different density of water in varying temperatures, along with the buoyancy effect, can create thermal stratification in the tank, which plays an important role in the performance of the tank. The design achievement is judged by how long it takes the tank to discharge the chilled water at the design temperature. The performance can be affected by many design parameters which make it difficult to analyze, and therefore is a good candidate for research. This paper shows how the full 3D numerical simulation and virtual design approach provide more detail and visualization of the flow field structure to improve the design. The main goal was to design the chilled water storage tanks to provide at least fifteen minutes of chilled water at a specific temperature for a data center during a power outage. Different octagonal inlet and outlet diffusers with different sizes and locations of the slots in the diffusers were virtually designed and their impacts on flow distribution, thermocline shape, swirl effect, and time amount of delivering cold water were investigated. The outcome was then used to optimize the design and provide solutions for improving the performance of the tank.

INTRODUCTION

Rack mounted information technology (IT) equipment located in data centers has grown exponentially in regards to electrical consumption and resultant heat output. Loading high densities has introduced the need for closely evaluating the potential loss of cooling capacity due to an interruption in normal electric power supply. With individual IT equipment racks generating 10 kilowatts of heat or more, even a short interruption in cooling has potentially negative consequences, due to the rapid increase in air temperature entering the IT equipment racks.

Most critical data centers have back-up electrical generation equipment to ensure the availability of power to IT areas as well as their supporting HVAC systems. However, there is a time delay between the loss of normal power, start-up of the back-up generator and transfer of power from normal to stand-by. Uninterruptible Power Systems (UPS) can be utilized to ensure that electrical power remains constant to sensitive equipment that cannot withstand even momentary power outages. The length of time for which the UPS systems are designed to provide power varies, but is typically in the range of 10-15 minutes for large data centers. The UPS allows critical IT equipment to be impervious to any blips in power supply until the back-up generation equipment is up and running.

R. Ghias is a Senior CFD Analyst, Y. Xu is an Energy Engineer II, R. Ellison is a Manager of Energy and Simulation, and C. Eisenhower is a Principal Engineer at Southland Industries, Dulles, Virginia

HVAC equipment, such as fans and pumps, can be connected to the UPS system so that they may also stay energized during the transition from normal to standby power. However, it is usually not cost effective to power larger loads such as centrifugal chiller compressors. Despite the mass in a chilled water system that could absorb some of the data center heat while the UPS connected HVAC equipment continues to run, the large loads inherent in such spaces would eventually result in an increase to the chilled water temperature and subsequent loss of cooling capability. One method to ensure that there is a sufficient buffer of chilled water available during this transition period is to use a Thermal Energy Storage (TES).

One choice of TES is to install such a tank on grade exterior to the Central Utility Plant (CUP) housing the chilled water generating equipment. There are some challenges with this approach such as temperature gains and energy consumption increases due to exposure to hot outdoor ambient, freezing issues in winter, air absorption to the system, security thread, and additional pump and control equipment. An alternative arrangement is to provide the TES via American Society of Mechanical Engineers (ASME) pressure rated tanks located inside the CUP. The tanks are inside a protected CUP and not exposed to outside ambient temperatures. Since the tanks are closed and rated for installation in the pressurized chilled water system, there are no issues with pressure control or air absorption.

However, the performance of these smaller tanks is not well documented. There are concerns that the water inside the tank will mix, not create good stratification, and therefore not provide the anticipated buffer of chilled water. The purpose of this Computational Fluid Dynamics CFD analysis was to investigate the performance of the tanks, and ensure that the system is capable of supplying the appropriate chilled water temperature for the duration of time dictated by the design parameters. In this case, it was decided to match the TES capacity with the approximate UPS battery life of fifteen minutes. It is critical to have confidence in the design of the TES system, since it will not be known whether the performance is deemed acceptable until the final Integrated Systems Testing (IST) has occurred. It will be costly to discover that the buffer is inadequate as the IST testing is the final step before turnover of the building to the user.

PREVIOUS WORKS AND NUMERICAL ANALYSIS

Many parameters can impact the performance of the tank, and a lot of experimental and numerical studies have been done to analyze these impacts (Karim 2009, Ghadar 1989, Bahnfleth 2003, Jabar 2011, Zurigat 1991, Stewart 1992). The design of the distribution system at the inlet and outlet are the most important impacts. However, despite several studies, more analysis is required in order to address the complex flow field and the impact of the design parameters on the stratification in the tank.

The inlet flow should distribute uniformly by the inlet diffuser and collect uniformly by the outlet diffuser in order to create the least disturbance and negative effect on natural stratification and performance of the tank. Earlier studies provide some recommendations and guidelines regarding the radial and octagonal diffusers. The Froude number (Fr) is a dimensionless parameter that is used as criteria in stratified thermal storage tank design. The Fr number is the ratio of the inertia force to the buoyancy force and Reynolds number is the ratio of the inertia force to the viscous force. The Fr and Re numbers can be defined as follows (Machie 1988):

$$Fr = \frac{u}{[g\beta(T_w - T_c)L]^{1/2}} \quad (1) \qquad Re = \frac{uL}{\nu} \quad (2)$$

Where u is the average velocity at the discharge slots of the inlet diffuser, it can be calculated based on the total flow rate and open area at the outlet of the diffuser. The gravitational acceleration is presented by g, ν is the kinematic viscosity, and β is the coefficient of volume expansion. T_w and T_c represent warm and cold water temperature in the tank, respectively, L is the characteristic dimension and varies based on the type of diffuser. For radial diffusers, it can be the distance between the disc and the top tank (top diffuser), while for circular or octagonal can be defined as the height of the openings above the top diffuser (Wildin 1989).

The study performed by Yoo et al. shows that when the Fr number is smaller or close to one, the buoyancy force dominates the inertia force but in many designs achieving this goal ends up to high pressure drop and needs to be considered during the design (Karim 2009). Hudson et al. (1979) found that a ratio of half between the total opening area in the diffuser branches to the cross sectional area of the corresponding branch pipe can help the flow uniformity. The low velocity at inlet slots is another key factor to keep buoyancy force dominant enough to effectively form the thermocline. Dorgan and Elleson (Dorgan 1994) investigated the swirling in the tank as a result of nonuniform velocity at diffuser slots and suggested that uniform static pressure in diffuser pipes can provide uniform discharge velocity at slots.

The comprehensive reviews and studies on radial and octagonal diffusers were performed by Dorgan and Elleson (Dorgan 1994) and Bahnfleth et al. (2003) respectively and readers are referred to the references mentioned for additional details.

In recent years, computational capabilities have increased and its relative costs have decreased significantly, making it affordable to perform full 3D simulation using computational fluid dynamics based software. Using such software to analyze complex phenomena and address the design challenges in the industry are not only able us to improve the design and performance of the system, but also make it possible to cut costs. This paper shows how employing a virtual approach and optimization can address the complexity of the flow field and provide practical solutions to improve the performance of the tank.

PROBLEM DEFINITION

As mentioned previously, Thermal Storage Tanks (TST) can be used to provide cooling capacity during a power outage in a data center. The main goal of the design was to provide cold water supply at 60° F (15.6° C) for at least 15 minutes. The inlet flow temperature to the tank was at 76° F (24.4° C) with a flow rate of (1540 GPM (97.16 lit/s)). Three tanks in the series were used to fulfill the requirements as a preliminary design. Figure 1(a) shows the schematic of the tanks. The maximum height and diameter of the tanks were 17 ft (5.58 m) and 12 ft (9.34 m) respectively, considering space restrictions of the indoor area.

Based on earlier research, (Will Bahnfleth ASHRAE 2003, Wildin 1985, Baines 1982, Cole 1982, Gross 1982) two double-ring diffusers were chosen to provide uniform flow distribution. Figure 1(b) shows the double-ring diffuser used in the top of the tank (charge) with different sized slots in inner and outer loops. The inlet pipe diameter was 12 inches.

CFD MODEL

The numerical simulations were performed using finite-volume based commercial software, which provides different turbulent models options and customization capabilities. The steady state solver was used in conjunction with optimization tools to design the proper charge and discharge diffusers and transient solver to design the tank and analyze the flow field and performance of the tank. More details in governing equations, turbulent models, boundary conditions, and optimization approaches are provided in the following sections.

Governing Equations and Turbulence Model

Reynolds-averaged Navier-Stokes equations along with two-equation turbulence models available in commercial iterative and control volume base solver were used for all numerical simulation performed in this paper. Control volume base solvers typically have less intrinsic numerical dissipations compare to finite element solvers. This makes it possible to capture more details of the flow field with same order of discretization in time and space. However, control volume base solvers are more sensitive to initial condition and need more skills to have a converged solution.

Based on previous studies in full-scale tank investigations (Bahnfleth & Musser 1999, Blevins 1984, Turner 1973), turbulent flow occurs close to the jets within up to the 10 nozzles width from the inlet. Also Will Bahnfleth (2003) used a realizable k-ε two-equation model with standard wall function for the near wall region and showed permissible results compared with the test. Moreover, they reported no major differences between the results of laminar flow and the corresponding turbulence model in an axisymmetric diffuser simulation. The realizable k-ε model has been used extensively in previous studies, and has been validated extensively especially for flows with jet and mixing layers (shih et al 1995). The enhanced wall treatment provides more accurate results with proper mesh resolution compared to standard wall functions by smoothly blending the logarithmic layer formulation with the laminar formulation (Kader 1981). The realizable k-ε with enhanced wall treatment near the wall regions was chosen based on previous studies.

NUMERICAL SIMULATION

Diffuser Design

It is required to perform full three dimensional simulations in order to capture the complex flow field in the diffuser pipes. The basic design was performed for double-ring octagonal diffusers with equal width discharge slots and an opening angle of 180 degrees.

There are many parameters that can affect diffuser design. The current design approach includes two steps. First step to find the proper pipe diameter ratio of the pipes that feed the inner and outer loops to keep a ratio of two to one between the flow rate of the outer and inner loops. Second step is to find the proper slots width on each branch of the loops in order to have a uniform flow distribution at discharge slots on each branch.

The criteria of ratio two between the outer and inner loops is based on the number of the discharge slots (4 and 8 on the inner and outer loops respectively) and the size of the inner and outer loops which have been determined to cover one third and two third of the cross section area of the tank in diffuser level respectively. The inner and outer loop diameters of the diffuser are 50 in (1.27 m) and 100 in (2.54 m) respectively.

i. Domain and Boundary Conditions

Figure 1(c) shows the domain and boundary conditions set up for the series of numerical simulations which were performed to find the optimized top and bottom diffuser in the tank.

The velocity at the inlet was calculated based on the inlet flow rate (1540 GPM (97.16 lit/s)). The outlet was set up as outlet pressure (zero gage pressure) which is far enough from the diffuser to eliminate the outlet boundary impact on discharge slots. A segregated scheme in steady state condition was used. Intensity and hydraulic diameter were used to specify the turbulence boundary conditions at inlet and outlet. The density was constant and all walls were assumed adiabatic (zero heat transfer). Tetrahedral and hexagonal mesh elements (~2.0 Million cells) with adequate refinement close to discharge slots were implemented in the domain. Figure 1(d) shows the mesh resolution on the diffuser and the rest of the domain.

ii. Optimization Results

The ratio of the inner and outer feeding pipes is the most effective factor on flow balance ratio between the inner and outer loops. The diameter of the inner feeding pipe was chosen as a parameter to perform series of simulations for design points in order to achieve the required flow balance ration. The outer feeding pipe diameter was held fixed at 6 inches. All slots had an equal width of 2 inches. Table 1 shows different inner diameters with corresponding mass flow ratio of outer to inner loops. The slot angle of 180° was chosen as for the design based on previous research (Will Bahnfleth ASHRAE 2003).

Table 1. The Inner Feeding Pipe Diameter vs. the Outer to Inner Loops Mass Flow Ratio

Inner feeding pipe diameter (in)[m]	Outer/inner mass flow ratio
2 [0.0508]	5.141
3 [0.0762]	2.035
4 [0.1016]	1.083
5 [0.1270]	0.649
6 [0.1524]	0.465

As a result, the inner feeding pipe with 3 inch diameter provided the overall mass flow rate ratio of two between the outer and inner loops. This ratio was chosen based on the ratio of the covered areas by the inner and outer loop at the cross section of the tank. However, further analysis showed that equal slot width does not satisfy balance mass flow rates on each branch of the inner and outer loops.

More analysis on the flow field within the diffuser shows that the size and location of the feeding pipes to the inner and outer loops have significant effect on mass flow balance in each branch. Figures 2(a) and 2(b) show that the negative

pressure (gage) makes the flow reverse into the diffuser, rather than discharging it out to the tank.

Figures 3(a), 3(b), and 3(c) show three other diffuser designs with different feeding pipe arrangements and their corresponding velocity magnitude contours at the cross sections of the loops. Even though adding more branches should create better flow balance in branches, the velocity contours in figure 3(a) shows that more flow is conducted to branches which are more aligned with feeding pipe direction and make the flow balance worse. Figure 3(b) shows the design in which the outer and inner loops receive the flow at the same time but the inner feeding pipe connection causing considerable reverse and unbalancing flow in the inner loop. Figure 3(c) shows the diffuser design that provides flow balance ratio of two between the outer and inner loops, but creates a considerable swirling effect in the tank due to the direction of the jets flow at discharge slots. The diffuser shown in figure 1(b) (3 and 6 inch diameter for inner and outer feeding loops) was selected to optimize for the best possible balanced flow on each of the branches within the loops. The slot width and distance from the feeding conjunction are two other important factors that impact on flow rate balance. The goal of the optimization was to achieve a mass flow ratio of one for the branches with and without feeding conjunctions using slot width as an input parameter. It is worth mentioning that the flow structures for the diffuser on top (discharging) and bottom (collecting) are different, which make it necessary to optimize each separately. Figures 4(a) and 4(b) show the optimized diffusers in the top and bottom of the tank. The discharge slots close to the feeding pipes in the outer loop have been relocated to avoid reverse flow in discharge slots. Also the slot angle for the top diffuser has been changes to 90° to reduce the swirling in the tank. Table 2 shows the mass flow ratio between the branches with and without conjunctions in inner and outer loops.

Table 2. The mass flow ratio between the branches with and without conjunctions in inner and outer loops

Location	Branch flow ratio
Inner loop top	1.27
Outer loop top	0.99
Inner loop bottom	1.03
Outer loop bottom	0.96

Tank Design

Even though proper design of the diffuser is necessary for stable thermocline in the storage tank, it does not guarantee it. Homan and Soo (1997) reported the internal wave motions cause reflective flow and eventually impact thermocline. Moreover, the shape of the tank, location and diameter of the inlet and outlet pipes, ratio of diffuser to tank radius, and the flow direction at discharge slots are additional factors that can affect thermocline as well as the performance of the tank. The optimized diffusers (explained in the previous section) were used in cylindrical tank to investigate the design impact on stratification and time period for which the tank can provide design cooling load.

i. Domain and Boundary Conditions

Figure 1(a) shows the domain and boundary conditions that have been used for tank simulation. The water inlet temperature was at 76° F (24.4° C) with velocity inlet based on design flow rate (1540 GPM (97.16 lit/s)). The density and viscosity were defined as functions of temperature to be able to capture buoyancy effect. The outlet pressure was considered for boundary condition at the outlet. Intensity and hydraulic diameter were used to specify the turbulence boundary conditions at inlet and outlet. There is a recharge flow (10 percent of the design flow rate) which keeps the temperature of the tank at 60° F (15.6° C) during the non-operational mode. The steady state flow field was used as an initial condition for the transient simulation at time= 0. The second order schemes were employed to solve the governing equations. The residual accuracy of $1.0e^{-4}$ was set up for all variables. The time step was ranged from 0.001 to 1 second to satisfy the residual criteria at each time step. The total size of the tetrahedral and hexagonal mesh elements was around 4.4 million cells for each tank. The simulation was run in parallel using 32 processors for three days in order to establish the results for first tank.

RESULTS AND DISCUSSION

A series of steady state simulations prior to transition simulation were performed to investigate the swirl effect on different diffuser arrangements. It was found that the swirl effect can be reduced by mounting baffle rings on the ceiling of the tank. Figure 5 shows the pathlines from the discharge slots in the inner and outer loops in a tank with and without mounted rings. The mounted rings break the big eddies into smaller ones and limit their transportation downstream in the tank. Smaller eddies create waves with higher frequency, which are dissipated faster than big eddies by viscosity. Another finding was that the maximum velocity magnitude at the horizontal cross section in the middle of the tank with rings was ~40 percent less than the maximum velocity in the same cross section of the tank with no rings. This provides more uniformity and stability of the thermocline within the tank. There were 6 baffle rings with height of 8 in (0.203 m) and were fully embedded in the water at the pressurized tank.

Figure 6 shows the instantaneous temperature contours at the vertical cross section in the middle of the tank with the baffles and optimized diffusers at different times. The warmer water (76° F (24.4° C)) enters the tank with high gradient temperature through the top diffuser. Due to the jets from the discharge slots, the inertial force dominates the buoyancy force and creates a mixing flow of cold and hot water close to the top diffuser figure 6(a). Further from the diffuser, the buoyancy force begins to overcome the inertial force and forms stratification of the water figure 6(b). The thermocline is fluctuating due to inertial waves and swirl effect. This fluctuation gets smaller as it gets farther from the top diffuser (figures 6(c) and 6(d)), and begins to amplify close to the diffuser at the bottom (figure 6(e)). A uniform collection of the flow at the bottom of the tank reduces the fluctuation and improves the stability of the thermocline (figure 6(f)). The total time between getting the warm water (76° F (15.6° C)) into the tank and going out was increased by 44 percent compared to using a similar diffuser with equal slots width and no baffles, which shows the impact of the optimization in the performance of the tank. It is worth to mention that the optimization of the tank could eliminate the need of third tank in the system and cut the cost and time in the project.

CONCLUSIONS

An affordable full three dimensional CFD analysis was used to investigate the performance of the thermal energy system for a data center. The results showed that the performance of the thermal storage energy has been improved significantly by employing the virtual design and optimization approach. It has been found that the size and location of the feeding pipes to the inner and outer loops can cause negative pressure at adjacent discharge slots and create non-uniform flow distribution. The flow direction at the slots can also be affected by the location of the feeding pipes. This can amplify the swirling in the tank and deteriorate thermal stratification phenomena within the tank. The negative impact of the swirling and wave motions in the tank can be alleviated by employing the mounted rings as baffles to break down the large eddies into small ones which dissipate faster and travel shorter in the tank. The size and location of the inlet and outlet pipes into and out of the tank can cause instabilities in the stratification and make short circuit between entrance and exit of the tank. This needs more investigation and analysis to be addressed properly.

REFERENCES

Abdul, J. N., Khalifa, A. T., Mustafa, and Farhan, A. K. 2011. Experimental study of temperature stratification in a thermal storage tank in the static mode for different aspect ratios. Journal of Energy and Applied Science, VOL. 6, NO. 2.

Bahnfleth, W. and Musser, A. 1999. Parametric study of charging inlet diffuser performance in stratified chilled water storage tanks with radial diffusers. ASHRAE research project 1077.

Bahnfleth, W., Song, J., and Cimbala, J. 2003. Measured and modeled charging of a stratified chilled water thermal storage tank with slotted pipe diffusers. International Journal of HVAC&R Research, 9 (4): 467-491.

Baines, W. D., Martin, W. W., and Sinclair, L.A. 1982. On the design of stratified water thermal storage tanks. ASHRAE Transactions, 88 (2): 426-439.

Blevin, R. 1984. Applied fluid dynamics handbook. New York: Van Nostrand Reinhold Company Inc.

Cole, R. L. and Bellinger, F. O. 1982. Thermally stratified tanks. ASHRAE Transactions, 88 (2): 1005-1017.
Dorgan, C.E. and Elleson, J.S. 1994. Design guide for cool thermal storage. ASHRAE Engineers. Atlanta, Ga.
Fluent Manual R14. ANSYS Inc.
Ghaddar, N. K., Al-Marafie, A. M., and Al-Kandari, A. 1989. Numerical simulation of stratification behavior in thermal storage tanks. Applied Energy, 32 (3): 225-239.
Gross, R. J. 1982. An experimental study of single medium thermocline thermal energy storage. ASME paper, 82-HT-53.
Homan, K., and Soo S. L. 1997. Model of the transient stratified flow into a chilled water storage tank. International Journal of Heat and Mass Transfer, 40(18): 4367-4377.
Hudson, H. E., Uhleer, R. B., and Bailey, R.W. 1979. Dividing flow manifolds with square edged laterals. Journal of Environmental Engineering, 105 (4): 745-755.
Kader, B. Temperature and concentration nprofiles in fully turbulent boundary layers. International Journal of Heat and Mass Transfer, 24 (9): 1541-1544.
Karim, M. A. 2009. Performance evaluation of a stratified chilled-water thermal storage system. World Academy of Science, 53: 326-334.
Machie, E. I. and Reeves, G. 1988. Stratified chilled-water storage design guide. EPRI Final report.
Shih, T.H., Liou, W., Shabbir, A., and Zhu, J. 1995. A new k-e eddy-viscosity model for high Reynolds number turbulent flows – model development and validation. Computer and Fluids, 24 (3): 227-238.
Stewart, W., Becher, B. and Cai, L. 1992. Downward impinging flows for stratified chilled water storage. Topics in Heat Transfer, 206 (2): 131-138.
Turner, J. 1973. Buoyancy effects in fluids. Cambridge University Press.
Wildin, M.W. and Truman, C.R. 1985. Evaluation of stratified chilled water storage techniques. EPRI report, EPRI. EM-4352.
Wildin, M.W., and Truman, C.R. 1989. Performance of stratified vertical cylindrical thermal storage tanks, part I: scale model tank. ASHRAE Technical Data Bulletin: 5 (3).
Yoo, J., Wildin, M. W., and Truman, C.R. 1986. Initial formation of a thermocline in simplified storage tanks. ASHRAE Transaction, 92 (2): 280-292.
Zurigat, Y., Liche, P., and Ghajar, A. 1991. Influence of inlet geometry on mixing in thermocline thermal energy storage. International Journal of Heat and Mass Transfer, 34: 115-125.

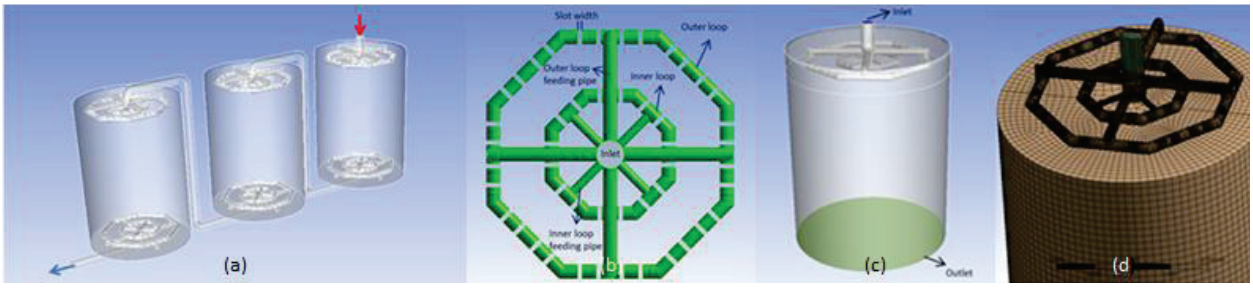

Figure 1 (a) Schematic of the tanks in preliminary design to provide cool water at 60° F for at least 15 minutes. (b) Schematic of the double-ring diffuser with different slot sizes which are highlighted on each branches of the inner and outer loops. (c) Set up boundary condition and domain for diffuser design. (d) A hybrid mesh generated with proper refinement in areas with high variable gradients.

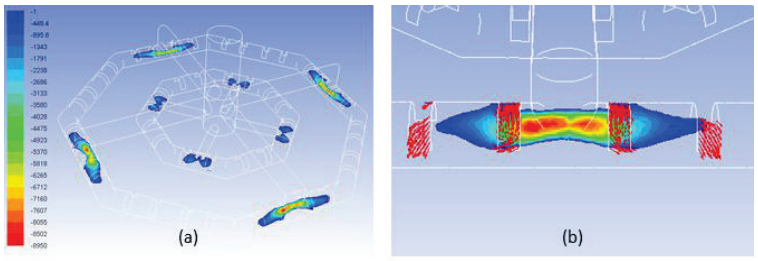

Figures 2 (a) The pressure contours show negative gage pressure in locations that feeding pipes are connected to inner and outer loops and as a result a reverse flow at slots close to the conjunctions (b) the inverse velocity vector in close up. Pressure unit is in Pascal.

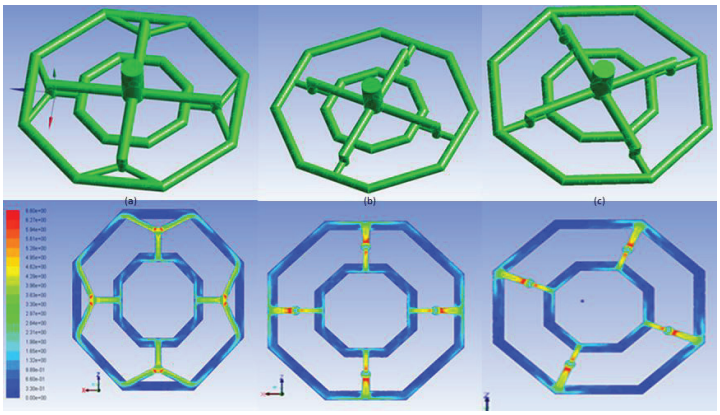

Figures 3 (a-c) Show three different feeding loop conjunction designs and corresponding velocity contours at middle cross section of the diffuser.

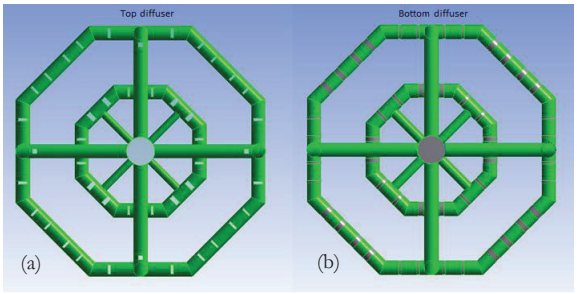

Figures 4 The optimized top (a) and bottom (b) diffuser that have been used in transient simulation of thermal storage tank.

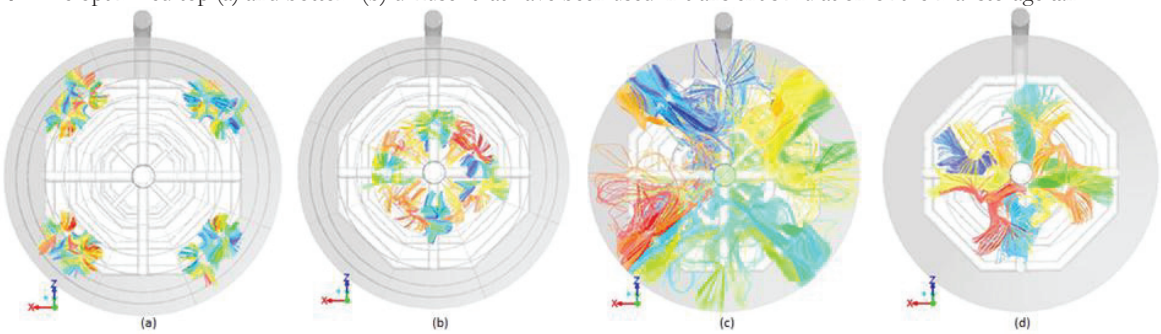

Figures 5 The pathlines form the inner and outer loops in the tank with the mounted rings on the ceiling of the tank (a) and (b) and the tank without rings (c) and (d).

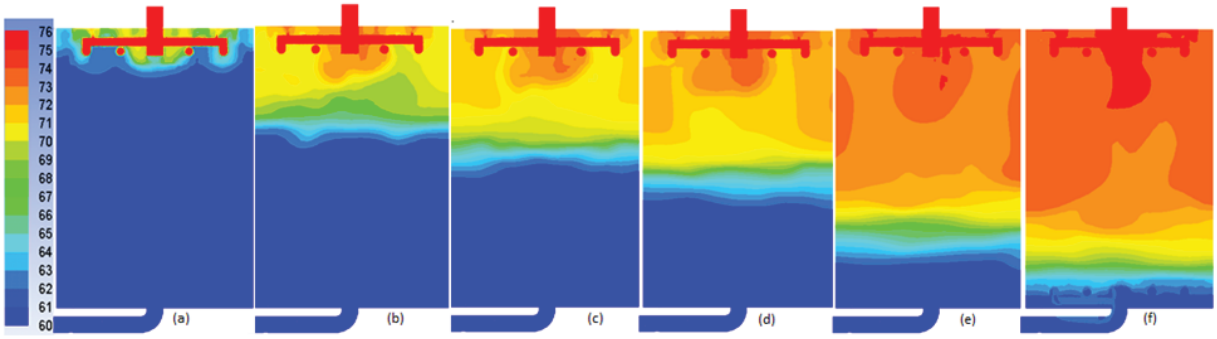

Figures 6 (a-f) Show the instantaneous temperature contours at the vertical cross section of the tank which varies from 60° to 76° F at 40, 140, 190, 240, 360, and 430 second respectively.